Int. J. Multiphase Flow, Vol. 2, pp. 113–138. Pergamon/Elsevier, 1975. Printed in Great Britain

BREAKUP OF EXTENDING LIQUID THREADS

T. MIKAMI,† R. G. COX and S. G. MASON‡

Pulp and Paper Research Institute of Canada and Department of Chemistry, McGill University, Montreal, Canada

(*Received* 31 *October* 1974)

Abstract—A theoretical and experimental study is made of the stability and breakup of an extending viscous liquid cylindrical thread suspended in an immiscible viscous liquid undergoing extensional flow.

It is shown that disturbances initiated as the thread is formed will in general as time proceeds be damped, then amplified and finally damped again. By considering disturbances being continually given to the system it is thus found that a disturbance which dominates at one moment will be completely different from that at any other. Assuming that breakup occurs when the disturbance amplitude becomes equal to cylinder radius, results are obtained for the time to breakup and for the final drop size resulting from breakup in terms of fluid properties, extension rate and the amplitude of disturbance given to system.

These results were confirmed by examining, with the aid of cinematography, the breakup of a liquid thread in hyperbolic flow.

INTRODUCTION

It is well known (Tomotika 1935, 1936; Rumscheidt & Mason 1961a, 1962; Goldsmith & Mason 1963; Goren 1962, 1964) that a cylindrical liquid thread suspended in a viscous medium, or a liquid annulus on a wire or on the inside of a tube, will develop small radial disturbances which grow until the eventual breakup into a multitude of droplets or rings. This phenomenon is of interest in connection with a variety of topics (emulsification of liquids, for example) and has been studied extensively for the case in which the fluids were at rest except for the small disturbances which were assumed to develop slowly.

On the other hand, Tomotika (1936) considered the growth of disturbances when the thread is continuously extended under conditions similar to those prevailing in axisymmetric extensional flow. He tested his theory using a few of Taylor's (1934) experimental results but the data were too limited to afford a conclusive test. In this paper, we study this phenomenon theoretically, showing how Tomotika's theory can be improved, and present confirming experimental data.

THEORETICAL PART

We consider an infinitely long neutrally buoyant liquid thread of radius a and viscosity η^* suspended in an immiscible liquid of viscosity η. The suspending fluid undergoes an axisymmetric extensional flow so that far away from the liquid thread, the flow velocity $\mathbf{u}$ with components in the cylindrical coordinate system (r, ϕ, z) illustrated in figure 1 tends to $\mathbf{U}$ given by

$$U_r = -\frac{1}{2}Gr, \quad U_\phi = 0, \quad U_z = Gz, \tag{1}$$

where U_r, U_ϕ and U_z are respectively the r-, ϕ- and z-components of velocity and G is the extension rate. We assume that the effect of inertia in the fluid is negligible compared with that of viscosity so that the velocity $\mathbf{u}$ outside and $\mathbf{u}^*$ inside the thread each satisfy the creeping motion equations. Since the velocity $\mathbf{U}$ defined in [1] satisfies identically the creeping motion equations

$$\nabla \cdot U = 0 \quad \text{and} \quad \eta \nabla^2 U - \nabla P = 0, \tag{2}$$

where the pressure P is constant and gives rise to stress components P_{ij} relative to the cylindrical coordinates given by

$$P_{rr} = -P + 2\eta \frac{\partial U_r}{\partial r} = -P - \eta G, \tag{3}$$

†On leave from Research Laboratories, Ashigara, FUGI Photo Film Co., Ltd., Minamiashigara, Kanagawa, Japan.
‡To whom enquiries should be addressed.

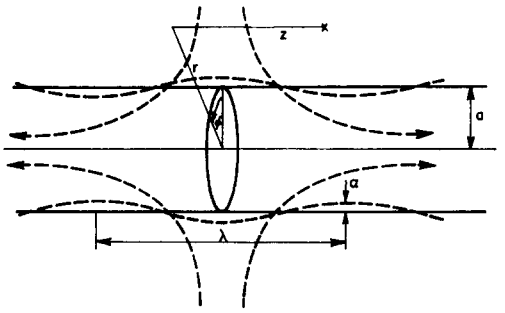

Figure 1. Cylindrical coordinates (r, ϕ, z) for the axisymmetric extensional flow; the direction of extension is the z-axis.

$$P_{zz} = -P + 2\eta \frac{\partial U_z}{\partial z} = -P + 2\eta G, \qquad [4]$$

$$P_{rz} = \eta\left(\frac{\partial U_z}{\partial r} + \frac{\partial U_r}{\partial z}\right) = 0, \qquad [5]$$

it is seen that the flow field inside and outside of the undeformed cylinder $r = a$ is in fact $\mathbf{U}$ everywhere, since it satisfies the required conditions of continuity of velocity and of tangential stress on $r = a$. However, since the normal stress difference is balanced by the interfacial tension γ, the constant pressures P^* inside and P outside the liquid cylinder are related by

$$(P^* + \eta^* G) - (P + \eta G) = \frac{\gamma}{a}. \qquad [6]$$

We will consider the growth of axisymmetric disturbances and take the cylinder to have a shape $r = a + \epsilon f(z, t)$, the disturbance flows being $\epsilon \mathbf{u}_1$ and $\epsilon \mathbf{u}_1^\dagger$ outside and inside the thread respectively, where ϵ is an arbitrary parameter $\ll 1$. Thus the total velocities are:

$$\mathbf{u}^* = \mathbf{U} + \epsilon \mathbf{u}_1^\dagger \quad \text{for } r < a + \epsilon f, \qquad [7]$$

$$\mathbf{u} = \mathbf{U} + \epsilon \mathbf{u}_1 \quad \text{for } r > a + \epsilon f. \qquad [8]$$

Since $\mathbf{U}$, $\mathbf{u}$ and $\mathbf{u}^*$ must individually satisfy the creeping motion equations, so must $\mathbf{u}_1$ and $\mathbf{u}_1^\dagger$.

Thus for $\mathbf{u}_1$ (and $\mathbf{u}_1^\dagger$)

$$\eta \nabla^2 \mathbf{u}_1 + \nabla p_1 = 0, \qquad [9a]$$

$$\nabla \cdot \mathbf{u}_1 = 0, \qquad [9b]$$

where p_1 is the pressure corresponding to $\mathbf{u}_1$. Defining the stream function ψ for $\mathbf{u}_1$ (and ψ^* for $\mathbf{u}_1^\dagger$):

$$(u_1)_r = \frac{1}{r}\frac{\partial \psi}{\partial z}, \quad (u_1)_z = -\frac{1}{r}\frac{\partial \psi}{\partial r} \qquad [10]$$

it follows from [9] that ψ (and ψ^*) satisfies the differential equation:

$$\left(\frac{\partial^2}{\partial r^2} - \frac{1}{r}\frac{\partial}{\partial r} + \frac{\partial^2}{\partial z^2}\right)\left(\frac{\partial^2}{\partial r^2} - \frac{1}{r}\frac{\partial}{\partial r} + \frac{\partial^2}{\partial z^2}\right)\psi = 0. \qquad [11]$$

We assume that the radial displacement f of the surface of the thread is of the form

$$f = \alpha \cos kz, \tag{12}$$

where α is the amplitude of the disturbance and k is the wave number related to the wave length λ by $k = 2\pi/\lambda$. The general solution to [11] which is consistent with the above form of f is found to be

$$\psi = \{C_1 rI_1(kr) + C_2 r^2 I_1'(kr) + C_3 rK_1(kr) + C_4 r^2 K_1'(kr)\} \sin kz \tag{13}$$

where $I_n(x)$ and $K_n(x)$ are modified Bessel functions of order n and argument x and C_1, C_2, C_3 and C_4 are all arbitrary functions of time t. The disturbance flow field must be finite everywhere and tend to zero as $r \to \infty$. Hence, the stream function for the outside liquid must be of the form

$$\psi = \{B_1 rK_1(kr) + B_2 r^2 K_1'(kr)\} \sin kz \tag{14}$$

while for the inner liquid,

$$\psi^* = \{A_1 rI_1(kr) + A_2 r^2 I_1'(kr)\} \sin kz \tag{15}$$

where A_1, B_1, A_2, B_2 are arbitrary functions of time to be determined by the following boundary conditions:

(1) The total velocities $\mathbf{u}^*$ and $\mathbf{u}$ are continuous on the deformed surface ($r = a + \epsilon f$) and hence since $\mathbf{U}$ is continuous there, so must be $\mathbf{u}_1$ and $\mathbf{u}^\dagger$. Thus

$$(u^\dagger)_r = (u_1)_r, \tag{16a}$$

$$(u^\dagger)_z = (u_1)_z \quad \text{on } r = a + \epsilon f. \tag{16b}$$

Since $\mathbf{u}^\dagger$ (and $\mathbf{u}_1$) can be written as expansions of the form:

$$(\mathbf{u}^\dagger)_{r=a+\epsilon f} = (\mathbf{u}^\dagger)_{r=a} + \epsilon f \left[\frac{\partial(\mathbf{u}^\dagger)}{\partial r}\right]_{r=a} + \cdots, \tag{17}$$

these boundary conditions, to the lowest order, take the form

$$(u^\dagger)_r = (u_1)_r, \tag{18a}$$

$$(u^\dagger)_z = (u_1)_z \quad \text{on } r = a. \tag{18b}$$

(2) The tangential stress is continuous on the deformed surface. Letting $\epsilon(p_1)_{ij}$ be the stress components corresponding to the disturbance flow $\epsilon\mathbf{u}_1$ outside the deformed cylinder $r = a + \epsilon f$, the total stress p_{ij} may be written

$$p_{ij} = P_{ij} + \epsilon(p_1)_{ij}, \tag{19}$$

which by the form of P_{ij} given by [3]–[5] yields

$$p_{rr} = -P - \eta G + \epsilon(p_1)_{rr}, \tag{20}$$

$$p_{zz} = -P + 2\eta G + \epsilon(p_1)_{zz}, \tag{21}$$

$$p_{rz} = \epsilon(p_1)_{rz}, \tag{22}$$

with similar expressions for the total stress inside $r = a + \epsilon f$ ($(p_1)_{ij}$ being replaced by $(p^\dagger)_{ij}$, the stress components corresponding to $\mathbf{u}^*$).

The hydrodynamic force F_i acting on an element of area of deformed surface $r = a + \epsilon f$ is

$$F_i = p_{ij} n_j, \tag{23}$$

where the outward normal $\mathbf{n}$ is from geometrical considerations,

$$(n)_z = -\epsilon \frac{\partial f}{\partial z} + 0(\epsilon^3), \tag{24}$$

$$(n)_r = \sqrt{[1-(n)_z^2]} = 1 + 0(\epsilon^2). \tag{25}$$

Hence

$$F_r = p_{rr}(n)_r + p_{rz}(n)_z = -P - \eta G + \epsilon (p_1)_{rr} + 0(\epsilon^2), \tag{26}$$

$$F_z = p_{zr}(n)_r + p_{zz}(n)_z = \epsilon (p_1)_{rz} + \epsilon P \frac{\partial f}{\partial z} - 2\eta G \epsilon \frac{\partial f}{\partial z} + 0(\epsilon^2). \tag{27}$$

The normal stress F_n and the tangential stress $\mathbf{F}_t$ on the deformed surface, $r = a + \epsilon f$ are given by

$$F_n = F_r(n)_r + F_z(n)_z = -P - \eta G + \epsilon (p_1)_{rr} + 0(\epsilon^2), \tag{28}$$

$$(\mathbf{F}_t)_z = F_z - F_n(n)_z$$

$$= \epsilon (p_1)_{rz} - 3\eta G \epsilon \frac{\partial f}{\partial z} + 0(\epsilon^2), \tag{29}$$

the boundary condition for continuity of tangential stress then yielding to lowest order:

$$(p^*)_{rz} - 3\eta^* G \frac{\partial f}{\partial z} = (p_1)_{rz} - 3\eta G \frac{\partial f}{\partial z} \quad \text{on } r = a + \epsilon f. \tag{30}$$

By expanding $(p^*)_{rz}$ and $(p_1)_{rz}$ about the undeformed surface $r = a$ in a manner similar to that for the velocity (see [17]) it is seen that this boundary condition [30] may be applied on $r = a$. The second term on each side of this equation was neglected by Tomotika (1936).

(3) Balance of the normal stress components by interfacial tension. If R_1 and R_2 are the principal radii of curvature of the deformed surface $r = a + \epsilon f = a + \epsilon\alpha \cos kz$, then

$$\frac{1}{R_1} = -\frac{\partial^2 r}{\partial z^2}\{1 + 0(\epsilon^2)\} = \epsilon\alpha k^2 \cos kz + 0(\epsilon^3), \tag{31}$$

$$\frac{1}{R_2} = \frac{1}{a + \epsilon\alpha \cos kz}\{1 + 0(\epsilon^2)\} = \frac{1}{a}\left(1 - \frac{\epsilon\alpha}{a}\cos kz\right) + 0(\epsilon^2), \tag{32}$$

and

$$\frac{1}{R_1} + \frac{1}{R_2} = \frac{1}{a} + \frac{\epsilon\alpha(k^2a^2 - 1)\cos kz}{a^2} + 0(\epsilon^2). \tag{33}$$

The normal stress boundary condition using the expression for the normal stress F_n given by [28] and neglecting terms of order ϵ^2 is given by

$$P^* + \eta^* G - \epsilon (p^*)_{rr} - P - \eta G + \epsilon (p_1)_{rr} = \frac{\gamma}{a} + \frac{\gamma\epsilon\alpha(k^2a^2 - 1)\cos kz}{a^2}. \tag{34}$$

Since the balance of the normal stress on the undeformed surface is given by [6], [34] becomes

$$(p^*_1)_{rr} - (p_1)_{rr} = \frac{\alpha\gamma}{a^2}(1 - k^2a^2)\cos kz. \qquad [35]$$

Using the values of ψ, ψ^* given by [14] and [15], the boundary conditions given by [18a], [18b], [30] and [35] may be expressed in the following forms

$$\begin{aligned}
&A_1kI_1(ka) + A_2kaI_1'(ka) - B_1kK_1(ka) - B_2kaK_1'(ka) = 0,\\
&A_1kI_0(ka) + A_2\{kaI_1(ka) + I_0(ka)\} + B_1kK_0(ka) - B_2\{kaK_1(ka) - K_0(ka)\} = 0,\\
&A_1(\eta^*/\eta)kI_1(ka) + A_2(\eta^*/\eta)kaI_0(ka) - B_1kK_1(ka) + B_2kaK_0(ka) = (3/2)[(\eta^*/\eta) - 1]G\alpha, \qquad [36]\\
&A_1(\eta^*/\eta)kI_1'(ka) + A_2(\eta^*/\eta)\{I_1'(ka) + kaI_1''(ka) - I_0(ka)\} - B_1kK_1'(ka)\\
&\quad - B_2\{K_1'(ka) + kaK_1''(ka) + K_0(ka)\} = \frac{\alpha\gamma}{2k\eta a^2}(1 - k^2a^2).
\end{aligned}$$

Next we shall calculate the change of amplitude α with time. At the deformed surface, $r = r(z, t)$, the radial velocity u_r is the rate of change (dr/dt) following a fluid particle which is given by

$$u_r = \frac{dr}{dt} = \frac{\partial r}{\partial t} + u_z\frac{\partial r}{\partial z}. \qquad [37]$$

Substituting [7] and $r = a + \epsilon\alpha\cos kz$ into [37] and neglecting terms in ϵ^2 yields

$$-\frac{1}{2}Ga - \frac{da}{dt} + \epsilon\left\{\left[A_1kI_1(ka) + A_2kaI_1'(ka) - \frac{1}{2}G\alpha - \frac{d\alpha}{dt}\right]\cos kz + \left[\alpha z\frac{dk}{dt} + G\alpha kz\right]\sin kz\right\} = 0, \qquad [38]$$

where the value of $(u^*_1)_r$ as calculated from the expression for ψ^* in [15] has been used. The term in ϵ^0 gives:

$$\frac{da}{dt} = -\frac{1}{2}Ga. \qquad [39]$$

Then if $a = a_0$ at $t = 0$

$$\frac{a}{a_0} = \exp\left(-\frac{1}{2}\int_0^t G\,dt\right). \qquad [40]$$

The term in ϵ^1 gives two equations:

$$\frac{dk}{dt} + Gk = 0, \qquad [41]$$

$$-\frac{1}{2}G\alpha + A_1kI_1(ka) + A_2kaI_1'(ka) = \frac{d\alpha}{dt}. \qquad [42]$$

Integration of [41] gives

$$\frac{k}{k_0} = \exp\left(-\int_0^t G\,dt\right), \qquad [43]$$

where $k = k_0$ at $t = 0$ and hence

$$\frac{\lambda}{\lambda_0} = \exp\left(\int_0^t G\,\mathrm{d}t\right), \tag{44}$$

λ_0 being the value of the wavelength λ at $t = 0$. The rate of change of the ratio of amplitude to thread radius α/a with time is

$$\frac{\mathrm{d}}{\mathrm{d}t}\left(\frac{\alpha}{a}\right) = \frac{1}{a}\left(\frac{\mathrm{d}\alpha}{\mathrm{d}t} - \frac{\alpha}{a}\frac{\mathrm{d}a}{\mathrm{d}t}\right), \tag{45}$$

which upon substituting [39] and [42] yields

$$\frac{\mathrm{d}}{\mathrm{d}t}\left(\frac{\alpha}{a}\right) = \frac{1}{a}[A_1 kI_1(ka) + A_2 kaI_1'(ka)]. \tag{46}$$

Solving next [36], which are now regarded as simultaneous linear equations for the four variables A_1, A_2, B_1 and B_2, we obtain A_1' and A_2 (to simplify we put $kA_1 = A_1'$, $kB_1 = B_1'$ and $x = ka$):

$$A_1' = \frac{1}{\Delta}\left\{\frac{\alpha\gamma}{2\eta a}(1-x^2)\Delta_1 - \frac{3}{2}\left(\frac{\eta^*}{\eta} - 1\right)G\alpha\bar{\Delta}_1\right\}, \tag{47}$$

$$A_2 = -\frac{1}{\Delta}\left\{\frac{\alpha\gamma}{2\eta a}(1-x^2)\Delta_2 - \frac{3}{2}\left(\frac{\eta^*}{\eta} - 1\right)G\alpha\bar{\Delta}_2\right\}, \tag{48}$$

where

$$\Delta = \left(\frac{\eta^*}{\eta}\right)xI_1'(x)\Delta_1 - \left(\frac{\eta^*}{\eta}\right)[(x^2+1)I_1(x) - xI_0(x)]\Delta_2 + xK_1'(x)\Delta_3 - [(x^2+1)K_1(x) + xK_0(x)]\Delta_4, \tag{49}$$

with Δ_1, Δ_2, Δ_3, Δ_4, $\bar{\Delta}_1$ and $\bar{\Delta}_2$ being

$$\Delta_1 = \begin{vmatrix} xI_1'(x) & K_1(x) & xK_1'(x) \\ I_0(x) + xI_1(x) & -K_0(x) & -K_0(x) + xK_1(x) \\ \left(\frac{\eta^*}{\eta}\right)xI_0(x) & K_1(x) & -xK_0(x) \end{vmatrix} \tag{50}$$

$$\Delta_2 = \begin{vmatrix} I_1(x) & K_1(x) & xK_1'(x) \\ I_0(x) & -K_0(x) & -K_0(x) + xK_1(x) \\ \left(\frac{\eta^*}{\eta}\right)I_1(x) & K_1(x) & -xK_0(x) \end{vmatrix} \tag{51}$$

$$\Delta_3 = \begin{vmatrix} I_1(x) & xI_1'(x) & xK_1'(x) \\ I_0(x) & I_0(x) + xI_1(x) & -K_0(x) + xK_1(x) \\ \left(\frac{\eta^*}{\eta}\right)I_1(x) & \left(\frac{\eta^*}{\eta}\right)xI_0(x) & -xK_0(x) \end{vmatrix} \tag{52}$$

$$\Delta_4 = \begin{vmatrix} I_1(x) & xI_1'(x) & K_1(x) \\ I_0(x) & I_0(x) + xI_1(x) & -K_0(x) \\ \left(\frac{\eta^*}{\eta}\right)I_1(x) & \left(\frac{\eta^*}{\eta}\right)xI_0(x) & K_1(x) \end{vmatrix} \tag{53}$$

$$\bar{\Delta}_1 = \begin{vmatrix} \left(\frac{\eta^*}{\eta}\right)[(x^2+1)I_1(x) - xI_0(x)] & xK_1'(x) & (x^2+1)K_1(x) + xK_0(x) \\ xI_1'(x) & K_1(x) & xK_1'(x) \\ I_0(x) + xI_1(x) & -K_0(x) & -K_0(x) + xK_1(x) \end{vmatrix} \quad [54]$$

$$\bar{\Delta}_2 = \begin{vmatrix} \left(\frac{\eta^*}{\eta}\right)xI_1'(x) & xK_1'(x) & (x^2+1)K_1(x) + xK_0(x) \\ I_1(x) & K_1(x) & xK_1'(x) \\ I_0(x) & -K_0(x) & -K_0(x) + xK_1(x) \end{vmatrix}. \quad [55]$$

Substituting [47] and [48] in [46] we get:

$$\frac{d}{dt}\left(\frac{\alpha}{a}\right) = \frac{\alpha\gamma}{2\eta a^2}(1-x^2)\Phi(x) - \frac{3G\alpha}{2a}\left(\frac{\eta^*}{\eta} - 1\right)\bar{\Phi}(x), \quad [56]$$

where

$$\Phi(x) = \frac{1}{\Delta}\{I_1(x)\Delta_1(x) - xI_1'(x)\Delta_2(x)\}, \quad [57]$$

$$\bar{\Phi}(x) = \frac{1}{\Delta}\{I_1(x)\bar{\Delta}_1(x) - xI_1'(x)\bar{\Delta}_2(x)\}. \quad [58]$$

Equation [56], which may be expressed as

$$\frac{d}{dt}\left(\ln\frac{\alpha}{a}\right) = \frac{\gamma}{2\eta a}(1-x^2)\Phi(x) - \frac{3}{2}G\left(\frac{\eta^*}{\eta} - 1\right)\bar{\Phi}(x), \quad [59]$$

may be solved for α/a to give

$$\frac{\alpha}{a}\Big/\frac{\alpha_0}{a_0} = \exp\int_0^t \left\{\frac{\gamma}{2\eta a}(1-x^2)\Phi(x) - \frac{3}{2}G\left(\frac{\eta^*}{\eta} - 1\right)\bar{\Phi}(x)\right\} dt, \quad [60]$$

where α_0 and a_0 are the values of α and a respectively at $t = 0$. From [40] and [43] we get

$$\frac{x}{x_0} = \left(\frac{k}{k_0}\right)\left(\frac{a}{a_0}\right) = \exp\left(-\frac{3}{2}\int_0^t G\, dt\right), \quad [61]$$

where $x_0 = k_0 a_0$ is the value of the dimensionless wave number x at $t = 0$. Then [40] may be written as

$$a = a_0\left(\frac{x}{x_0}\right)^{1/3}, \quad [62]$$

which when substituted into [60] gives

$$\frac{\alpha}{\alpha_0} = \left(\frac{x}{x_0}\right)^{1/3} \exp\int_0^t \left\{\frac{\gamma x_0^{1/3}}{2\eta a_0}x^{-1/3}(1-x^2)\Phi(x) - \frac{3}{2}G\left(\frac{\eta^*}{\eta} - 1\right)\bar{\Phi}(x)\right\} dt, \quad [63]$$

where both x and G are functions of time t. If G is constant, then

$$x = x_0 \exp\left(-\frac{3}{2}Gt\right), \quad [64]$$

the value of α/α_0 given by [63] then being expressible as

$$\ln\frac{\alpha}{\alpha_0}=\frac{\gamma x_0^{1/3}}{3\eta a_0 G}\int_x^{x_0} x^{-4/3}(1-x^2)\Phi(x)\,dx-\left(\frac{\eta^*}{\eta}-1\right)\int_x^{x_0} x^{-1}\bar{\Phi}(x)\,dx+\frac{1}{3}\ln\left(\frac{x}{x_0}\right), \qquad [65]$$

giving the fractional change of amplitude of disturbances on the surface of the liquid thread being elongated in the steady axisymmetric extensional flow.

Amplitude α

Equation [65] gives the value of α/α_0 as a function of η^*/η, $\gamma/\eta G a_0$, x_0 and x. Calculations of the variation of $\ln \alpha/\alpha_0$ with $x(\leq x_0)$ for various values of x_0 and $\gamma/\eta G a_0$, and for three values of η^*/η ($=1.0$, 10^{-3} and 10^2) were performed, typical results being shown in figure 2. Details of this

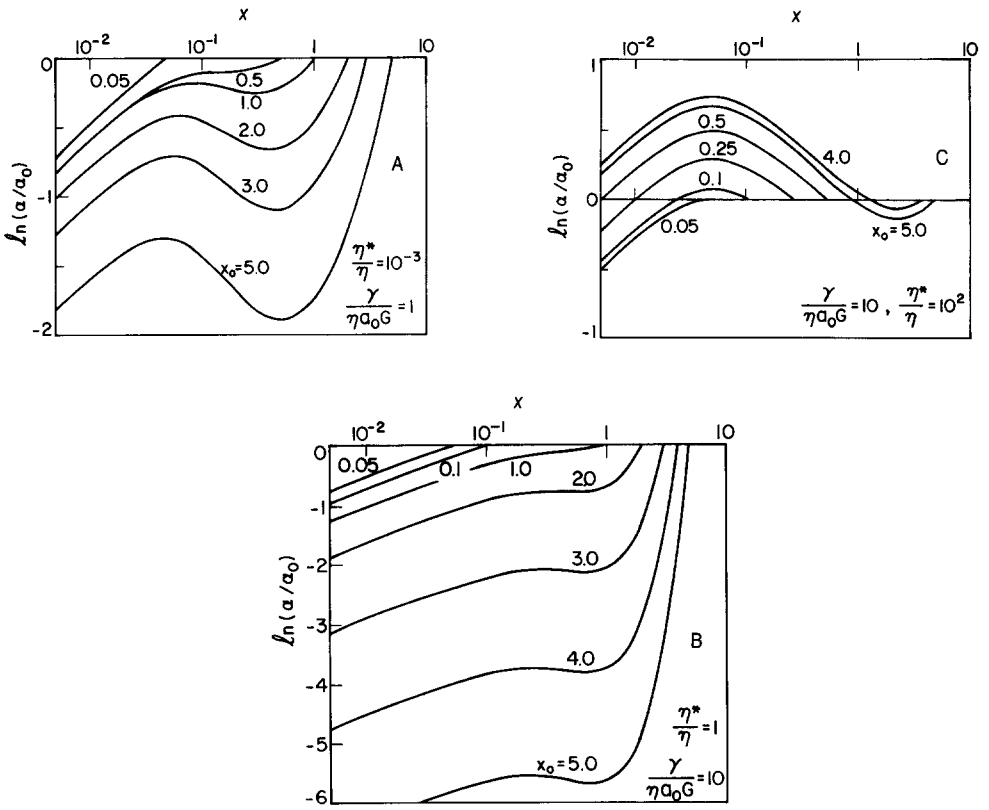

Figure 2. Calculated values of $\ln \alpha/\alpha_0$ against x for (A) $\eta^*/\eta = 10^{-3}$, $\gamma/\eta a_0 G = 1.0$, (B) $\eta^*/\eta = 1.0$, $\gamma/\eta a_0 G = 10.0$ and (C) $\eta^*/\eta = 10^3$, $\gamma/\eta a_0 G = 10.0$. The numbers designate values of the initial wave number x_0.

calculation are given in appendix II. It is clear from these results that $\ln \alpha/\alpha_0$ for large x_0, say $x_0 > 5.0$, initially decreases with time (i.e. as x decreases from $x = x_0$) and after passing through a minimum value denoted by $\ln \alpha_m/\alpha_0$, begins to increase and then finally decrease again. However for very small x_0, say $x_0 = 0.05$, $\ln \alpha/\alpha_0$ decreases monotonically for all time. This means that for large x_0, the disturbance whose initial amplitude is α_0 is damped in the initial stage of the extension, but at a later stage is amplified and at a still later stage is damped again. Thus some disturbances grow while at the same time others decay.

Since the functions $\Phi(x)$ and $\bar{\Phi}(x)$ each behave like $x^2 \ln x$ as x tends to 0 [appendix I-A], the integrals in [65] are convergent as x tends to 0 thus showing that $\ln \alpha/\alpha_0 \sim 1/3 \ln (x/x_0)$ as $x \to 0$. Thus for every x_0, $\ln \alpha/\alpha_0$ decreases to $-\infty$ as $x \to 0$, this behaviour being evident in figure 2.

It can also be seen in figure 2 that for x_0 sufficiently large, that $\ln (\alpha/\alpha_0)$ has a minimum value

$\ln(\alpha_m/\alpha_0)$ occurring at a value of x (denoted by x_m) which approaches unity as x_0 tends to infinity. This behaviour can be proved theoretically as follows. The asymptotic form of the functions $\Phi(x)$ and $\bar{\Phi}(x)$ as $x \to \infty$ are (appendix I-B)

$$\Phi(x) \sim \left(1+\frac{\eta^*}{\eta}\right)^{-1} x^{-1}, \qquad [66]$$

$$\bar{\Phi}(x) \sim -\frac{1}{2}\left(1+\frac{\eta^*}{\eta}\right)^{-1} x^{-1}. \qquad [67]$$

Thus as $x_0 \to \infty$ [with $x = 0(1)$]

$$\int_x^{x_0} x^{-4/3}(1-x^2)\Phi(x)\,dx \sim -\frac{3}{2}\left(1+\frac{\eta^*}{\eta}\right)^{-1} x_0^{2/3} + f(x), \qquad [68]$$

$$\int_x^{x_0} x^{-1}\bar{\Phi}(x)\,dx \sim g(x) \qquad [69]$$

where $f(x)$, $g(x)$ are functions of x only. Hence as $x_0 \to \infty$

$$\ln\left(\frac{\alpha}{\alpha_0}\right) \sim \left[\frac{\gamma x_0^{1/3}}{3\eta a_0 G}\left\{-\frac{3}{2}\left(1+\frac{\eta^*}{\eta}\right)^{-1} x_0^{2/3} + f(x)\right\}\right] - \left(\frac{\eta^*}{\eta}-1\right)g(x) + \frac{1}{3}(\ln x - \ln x_0), \qquad [70]$$

the first term of which is dominant. Hence for $x_0 \to \infty$, $\ln(\alpha/\alpha_0)$ can be approximated by:

$$\ln\left(\frac{\alpha}{\alpha_0}\right) = \frac{\gamma x_0^{1/3}}{3\eta a_0 G}\int_x^{x_0} x^{-4/3}(1-x^2)\Phi(x)\,dx. \qquad [71]$$

Thus for large x_0,

$$\frac{d}{dx}\ln\left(\frac{\alpha}{\alpha_0}\right) = -\frac{\gamma x_0^{1/3}}{3\eta a_0 G} x^{-4/3}(1-x^2)\Phi(x), \qquad [72]$$

yielding

$$\frac{d}{dx}\ln\left(\frac{\alpha}{\alpha_0}\right) = 0 \quad \text{and} \quad \frac{d^2}{dx^2}\ln\left(\frac{\alpha}{\alpha_0}\right) > 0 \quad \text{at } x = 1. \qquad [73]$$

Hence $\ln(\alpha/\alpha_0)$ has a minimum at $x = x_m$ for x_0 sufficiently large, the value of $x_m \to 1$ as $x_0 \to \infty$. Thus for x_0 sufficiently large the behaviour of $\ln(\alpha/\alpha_0)$ is always such that as x decreases, it initially decreases to a minimum at $x = x_m$ ($\simeq 1$) and then increases, only to decrease to $-\infty$ as $x \to 0$. However, as already noted $\ln(\alpha/\alpha_0)$ will, for small x_0, decrease monotonically as x decreases. This can be proved by noting that from the behaviour of $\Phi(x)$ and $\bar{\Phi}(x)$ as $x \to 0$, the integrals in [65] tend to zero as x_0 (and hence x) $\to 0$. Thus $\ln(\alpha/\alpha_0) \sim 1/3 \ln(x/x_0)$ as $x_0 \to 0$, which decreases monotonically as x decreases from x_0 to 0. In this case x_m is defined to be zero. Thus there is a critical value of x_0 above which $\ln(\alpha/\alpha_0)$ has a minimum value and below which $\ln(\alpha/\alpha_0)$ has no minimum value, that is to say, the disturbance is damped out for all time. This critical value of x_0 was found to increase as $\gamma/\eta G_0 a$ decreases for all η^*/η calculated.

Magnification of amplitude α

We shall now investigate the magnification of disturbances which are assumed to be continuously initiated during the extension of the liquid thread and assume that the amplitude of such disturbances to the system is independent of the radius of the liquid thread and of the

disturbance wave length. Thus at any given time the wave with given wave number $x = x_0 \exp(-3/2)Gt$ for which $x < x_m$ and $\alpha > \alpha_m$ which has greatest amplitude is that which starts at a time corresponding to $x = x_m$.

Thus the magnification M of a disturbance is

$$\text{(i)}\quad M = \ln(\alpha/\alpha_0) - \ln(\alpha_m/\alpha_0) = \ln(\alpha/\alpha_m) \quad \text{for } x < x_m,\ \alpha > \alpha_m \qquad [74a]$$

$$\text{(ii)}\quad M = 0 \quad \text{for } x < x_m,\ \alpha < \alpha_m \qquad [74b]$$

(This is the case of a disturbance initiated at x_m which has been amplified and then damped to less than its original amplitude.)

$$\text{(iii)}\quad M = 0 \quad \text{for } x > x_m \qquad [74c]$$

(This is the case of a disturbance which up to the present time has been continuously damped.)

This magnification, M, will, at a given time, be a function of x_0, the initial dimensionless wave number. Figure 3 shows the results of the calculation of the magnification M as a function of x_0 for various fixed values of Gt for typical values of the parameters ($\eta^*/\eta = 10^{-3}$ and $\gamma/\eta a_0 G = 1.0$). For a given value of Gt the magnification takes a maximum value at $x_0 = (x_0)_{opt}$. This $(x_0)_{opt}$ which is the initial wave number whose disturbance has the largest amplitude at time t, is different at different times.

That a maximum for M always occurs (unless M is identically zero for all x_0) for a fixed t can be shown by noting that:

(i) as x_0 tends to 0 (so that x also tends to 0),

$$\ln \alpha/\alpha_0 \sim 1/3 \ln(x/x_0) \qquad [75]$$

representing a disturbance which always dies away for all time so that $x_m = 0 < x$, giving $M = 0$.

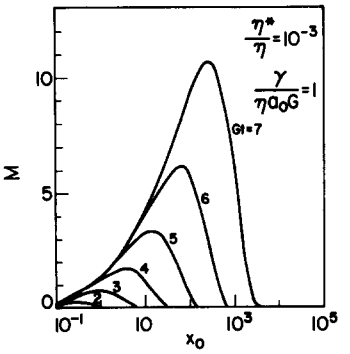

Figure 3. Calculation of the magnification M as a function of x_0 for various fixed values of Gt for $\eta^*/\eta = 10^{-3}$ and $\gamma/\eta a_0 G = 1.0$.

(ii) as x_0 tends to ∞, $x = x_0 \exp(-3/2Gt)$ also tends to ∞ for fixed t, and hence from the asymptotic forms of the functions $\Phi(x)$, $\bar{\Phi}(x)$ given by [66] and [67],

$$\ln \alpha/\alpha_0 \sim \frac{\gamma}{2\eta a_0 G}\left(1+\frac{\eta^*}{\eta}\right)^{-1}(x_0^{1/3}x^{2/3} - x_0). \qquad [76]$$

Thus $\ln(\alpha/\alpha_0)$ increases monotonically with x if x_0 and x are large. Thus $x > x_m$, and hence $M = 0$.

Therefore M has a maximum unless $\mathrm{d}/\mathrm{d}x\ (\ln \alpha/\alpha_m)$ is positive for all values of x in $x_0 \exp(-3/2Gt) < x < x_0$ for all $x_0 > 0$ in which case $M = 0$ for all x_0 for the particular time considered.

Figure 4A shows how this maximum magnification M_{max} varies with η^*/η for a given $\gamma/\eta a_0 G = 10^2$. It is clear that it takes a longer time to arrive at a particular M_{max} for large η^*/η than for small η^*/η. As Gt tends to 0, $(x_0)_{opt}$ tends to values which have already been calculated by Tomotika (1935) for the case of the stationary liquid cylinder, namely 0.257, 0.563 and 0.243 for $\eta^*/\eta = 10^{-3}$, 1.0 and 10^2 respectively. This occurs since the chosen value of $\gamma/\eta a_0 G$ is large. Figure 4B shows similarly the effect of $\gamma/\eta a_0 G$ on M_{max} for given $\eta^*/\eta = 10^{-3}$. It is clear that disturbances grow more slowly for small $\gamma/\eta a_0 G$ than for large. As Gt tends to 0 with $\gamma/\eta a_0 G$ sufficiently large, $(x_0)_{opt}$ tends to Tomotika's value of 0.257 for this case ($\eta^*/\eta = 10^{-3}$).

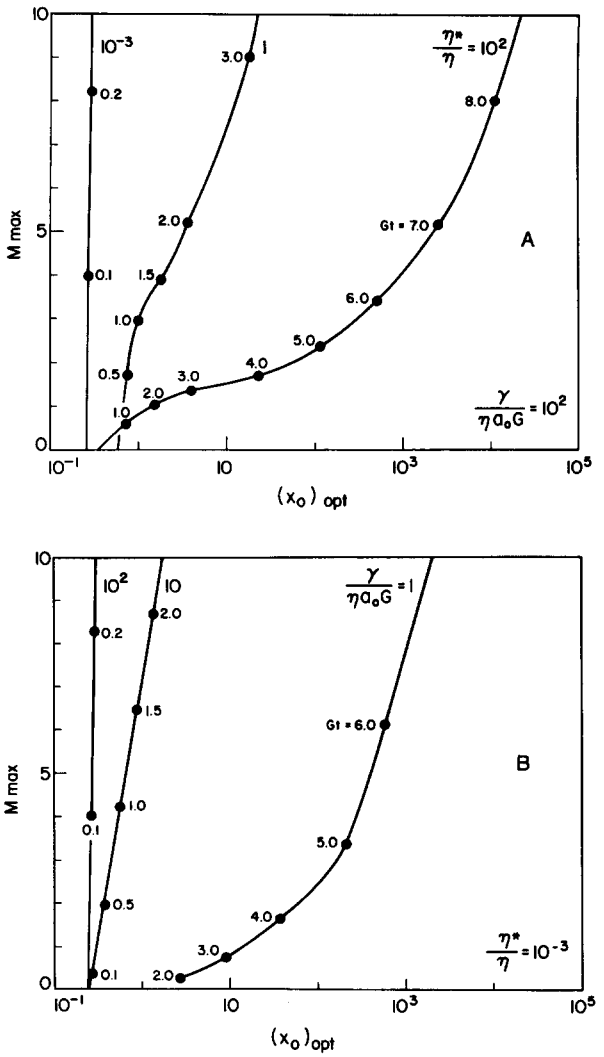

Figure 4. Values of M_{max} and $(x_0)_{opt}$ for (A) various values of Gt and η^*/η with $\gamma/\eta a_0 G = 10^2$, (B) various values of Gt and $\gamma/\eta a_0 G$ with $\eta^*/\eta = 10^{-3}$.

The values $x_{opt} = (x_0)_{opt} \exp(-3/2Gt)$ of the wave number at time t for the disturbance of maximum amplitude can be determined as a function of Gt for various values of $\gamma/\eta a_0 G$ and η^*/η. These results, shown in figure 5, give values of x_{opt} at $Gt = 0$ which agree in the limit of $\gamma/\eta a_0 G \to \infty$ with the values calculated by Tomotika for the stationary case. As Gt increases, x_{opt} decreases to an asymptotic value, this decrease being most rapid when $\gamma/\eta a_0 G$ is large. The calculated amplitude for $\gamma/\eta a_0 G = 1.0$, $\eta^*/\eta = 10^{-3}$ and for $\gamma/\eta a_0 G = 10.0$, $\eta^*/\eta = 1.0$, for small x_0 did not take any minimum value as shown in figure 2A,B, this resulting in M being identically zero for all x_0 with Gt small. For still smaller values of $\gamma/\eta a_0 G$, [$\gamma/\eta a_0 G = 10^{-1} \sim 10^{-3}$, $\eta^*/\eta = 10^{-3}$ and for $\gamma/\eta a_0 G = 1 \sim 10^{-3}$, $\eta^*/\eta = 1.0$], the calculated amplitude did not take any

minimum value for $Gt \leq 10$. This is why in figure 5A and figure 5B there are no calculated data for these values of $\gamma/\eta a_0 G$.

We now calculate the asymptotic value of x_{opt} for $Gt \to \infty$. In this limit $x \ll x_0$ since $x = x_0 \exp(-3/2Gt)$. Thus the magnification M will be greater than zero only if $x_0 \gg 1$ since x_0 of order unity with x small would imply that $\ln \alpha/\alpha_0 \sim 1/3 \ln (x/x_0)$ yielding $M = 0$. Furthermore, one must also have x of order unity since $d/dx\ (\ln \alpha/\alpha_0)$ is positive ($M = 0$) for large x and x_0. This case involving $x_0 \to \infty$ ($x = 0(1)$) has already been discussed (see [68]–[71]) and thus we obtain in the limit $Gt \to \infty$,

$$\ln\left(\frac{\alpha}{\alpha_0}\right) \simeq \frac{\gamma}{3\eta a_0 G} x_0^{1/3} \int_x^{x_0} x^{-4/3}(1-x^2)\Phi(x)\,dx. \qquad [77]$$

This has a minimum at $x = 1$, giving

$$M = \ln\left(\frac{\alpha}{\alpha_0}\right) - \ln\left(\frac{\alpha}{\alpha_m}\right)$$

$$= \frac{\gamma}{3\eta a_0 G} x_0^{1/3} \int_{x_0 e^{-3/2Gt}}^{1} x^{-4/3}(1-x^2)\Phi(x)\,dx, \qquad [78]$$

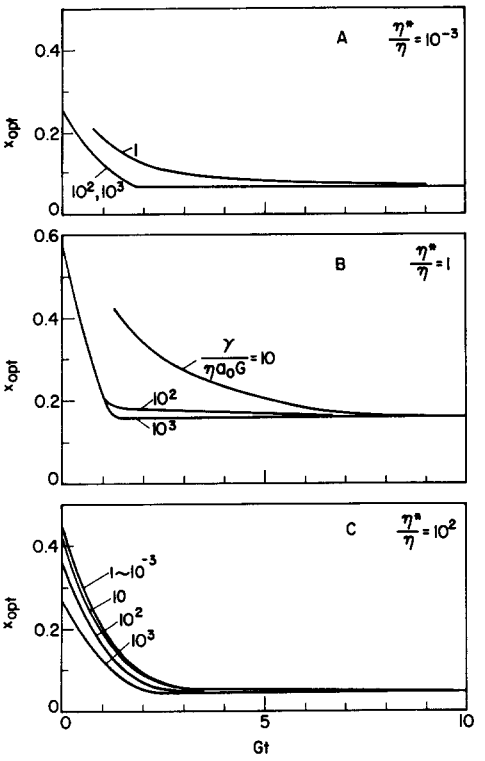

Figure 5. Calculated values of $x_{opt} = (2\pi a/\lambda)_{opt}$ against Gt for (A) $\eta^*/\eta = 10^{-3}$, (B) $\eta^*/\eta = 1$, and (C) $\eta^*/\eta = 10^2$ for various values of $\gamma/\eta a_0 G$. The numbers designate $\gamma/\eta a_0 G$.

where we have written $x = x_0 \exp(-3Gt/2)$. If we write

$$f(x) = \int_x^1 x^{-4/3}(1-x^2)\Phi(x)\,dx, \qquad [79]$$

then

$$M = \frac{\gamma}{3\eta a_0 G} x_0^{1/3} f(x_0 e^{-3Gt/2}). \qquad [80]$$

For fixed Gt, M has a maximum value when $dM/dx_0 = 0$ or

$$f(x_0 e^{-3Gt/2}) + 3x_0 e^{-3Gt/2} f'(x_0 e^{-3Gt/2}) = 0. \quad [81]$$

Letting y_* be the root of

$$f(y_*) + 3y_* f'(y_*) = 0, \quad [82]$$

we see that

$$x_0 e^{-3Gt/2} = y_*, \quad [83]$$

giving

$$x_{opt} = y_*. \quad [84]$$

Therefore, as Gt tends to infinity, $x_{opt} = (2\pi a/\lambda)_{opt}$ tends to a constant value, y_*, where

$$\int_{y_*}^{1} x^{-4/3}(1-x^2)\Phi(x)\,dx - 3y_*^{-1/3}(1-y_*^2)\Phi(y_*) = 0. \quad [85]$$

This value of y_* is independent of $\gamma/\eta a_0 G$ but does depend on η^*/η since $\Phi(x)$ depends on only η^*/η.

Calculated values of the variation of y_* with η^*/η are shown in figure 6. It is interesting to see that x_{opt} $(= y_*)$ takes maximum value $y_{*,max} = 0.185$ at $\eta^*/\eta = 0.14$ in a manner similar to the stationary case ($x_{opt,max} = 0.589$ at $\eta^*/\eta = 0.28$). The asymptotic values of x_{opt} obtained for $\eta^*/\eta = 10^{-3}$, 1.0 and 10^2 [0.0670, 0.161 and 0.0440 respectively] agree with values shown in figure 5. We have considered above, the conditions for maximization of $\ln(\alpha/\alpha_0)$ instead of $\ln[(\alpha/a)/(\alpha_0/a_0)]$ as considered by Tomotika (1936). Thus while we have considered a disturbance with an initial amplitude α_0 independent of column radius and disturbance wave length, Tomotika assumed an initial amplitude α_0 proportional to a_0/a which would therefore be varying with time.

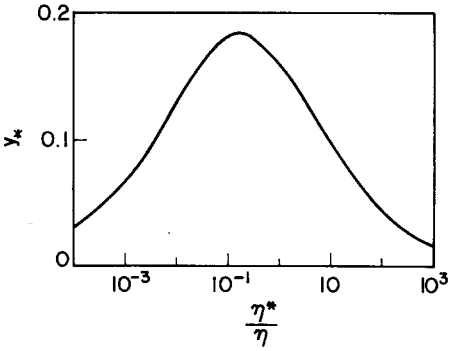

Figure 6. The values of y_* (i.e. x_{opt} at $Gt = \infty$) as a function of η^*/η.

Size of drop after breakup

Assuming that the extending liquid thread breaks up when the amplitude of the disturbance which has the largest magnification at a given time t becomes equal to the thread radius, it is possible to calculate this time t (denoted by t_b) and also to calculate the radius of drop R produced by breakup by using conservation of volume:

$$\frac{R}{a_0} = \left(\frac{3\pi}{2}\right)^{1/3} (x_{opt})^{-1/3} e^{-Gt_b/2}, \quad [86]$$

or in the limit $Gt_b \to \infty$

$$\frac{R}{a_0} \sim \left(\frac{3\pi}{2}\right)^{1/3} (y*)^{-1/3} e^{-Gt_b/2}. \qquad [87]$$

Values of R/a_0 against Gt_b for various values of $\gamma/\eta a_0 G$ are plotted in figure 7 for $\eta^*/\eta = 10^{-3}$, 1.0 and 10^2. In all cases the particle radius, R/a_0, decreases with the increase of Gt_b, the value of R/a_0 becoming independent of $\gamma/\eta a_0 G$ at sufficiently large Gt_b taking the value given by [87] (indicated as broken lines). At a given Gt_b and $\gamma/\eta a_0 G$, R/a_0 takes a smaller value for $\eta^*/\eta = 1.0$ than for $\eta^*/\eta = 10^{-3}$ or 10^2 because x_{opt} in [86] take a larger value for $\eta^*/\eta = 1.0$ than that for $\eta^*/\eta = 10^{-3}$ or 10^2.

We define $\epsilon \ll 1$ as the ratio (α_m/a_0) of the disturbance amplitude (which was assumed to originate at $x = x_m$) to the initial column radius. Then

$$\ln \epsilon = \ln\left(\frac{\alpha_m}{\alpha}\frac{\alpha}{a}\frac{a}{a_0}\right) \qquad [88]$$

which at breakup $[\alpha/a = 1.0]$ gives

$$\ln \epsilon^{-1} = \ln \frac{\alpha_b}{\alpha_m} + \frac{1}{2} Gt_b. \qquad [89]$$

Substituting $x_b = x_0 \exp(-3/2Gt_b)$, we get

$$\ln \epsilon^{-1} = \ln\left(\frac{\alpha_b}{\alpha_m}\right) - \frac{1}{3}\ln\left(\frac{x_b}{x_0}\right), \qquad [90]$$

where we are considering the wave causing breakup. Thus

$$x_0 = (x_0)_{opt}, \qquad [91]$$

$$x_b = (x_0)_{opt} \exp\left(-\frac{3}{2}Gt_b\right), \qquad [92]$$

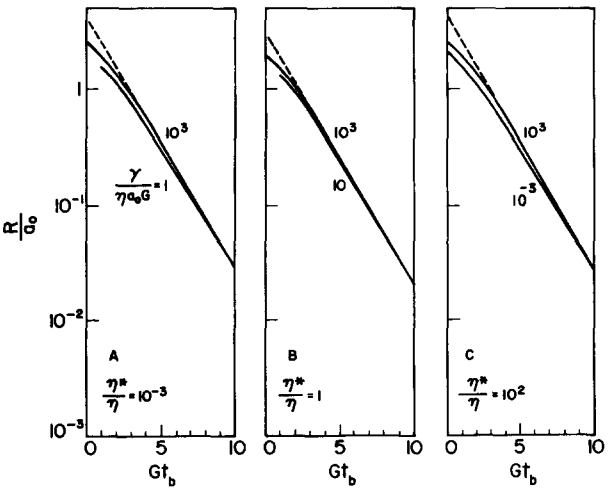

Figure 7. R/a_0 against Gt_b for (A) $\eta^*/\eta = 10^3$, (B) $\eta^*/\eta = 1$, and (C) $\eta^*/\eta = 10^2$, for various $\gamma/\eta a_0 G$. The numbers designate $\gamma/\eta a_0 G$ and the broken lines the asymptotic values for large Gt_b given by [87].

giving

$$\ln \epsilon^{-1} = \frac{\gamma}{3\eta a_0 G}(x_0)_{\text{opt}}^{1/3} \int_{(x_0)_{\text{opt}}}^{x_m} e^{-Gt_b/2} \cdot \quad x^{-4/3}(1-x^2)\Phi(x)\,dx - \left(\frac{\eta^*}{\eta} - 1\right) \int_{(x_0)_{\text{opt}}}^{x_m} e^{3Gt_b/2} \quad x^{-1}\bar{\Phi}(x)\,dx$$
$$+ \frac{1}{3} \ln \frac{(x_0)_{\text{opt}}}{x_m}, \qquad [93]$$

where x_m is the value of x at minimum amplitude for $x_0 = (x_0)_{\text{opt}}$. Calculated values of $\ln \epsilon^{-1}$ against Gt_b for various values of $\gamma/\eta a_0 G$ are plotted in figure 8 for $\eta^*/\eta = 10^{-3}$, 1.0 and 10^2 respectively. From these results we can see that for a given ϵ it takes longer time for the liquid thread to breakup for smaller values of $\gamma/\eta a_0 G$ and also for larger values of η^*/η.

An upper bond for t_b is obtained by noting that

$$a_b = a_0 e^{-Gt_b/2} > \alpha_m,$$

since if $a_b < \alpha_m$ we have an impossibility as the thread would already have broken up. Thus

$$Gt_b < 2 \ln a_0/\alpha_m. \qquad [94]$$

This upper bound of Gt_b is plotted as $-\cdot-\cdot-$ line in figure 8. As Gt tends to infinity, $x_m \sim 1$ and $(x_0)_{\text{opt}} \sim y_* e^{3Gt_b/2}$, yielding

$$\ln \epsilon^{-1} \sim \frac{\gamma}{3\eta a_0 G}(y_*)^{1/3} e^{Gt_b/2} \int_{y_*}^{1} x^{-4/3}(1-x^2)\Phi(x)\,dx - \left(\frac{\eta^*}{\eta} - 1\right) \int_{y_*}^{1} x^{-1}\bar{\Phi}(x)\,dx + \frac{1}{3} \ln y_* + \frac{1}{2} Gt_b. \qquad [95]$$

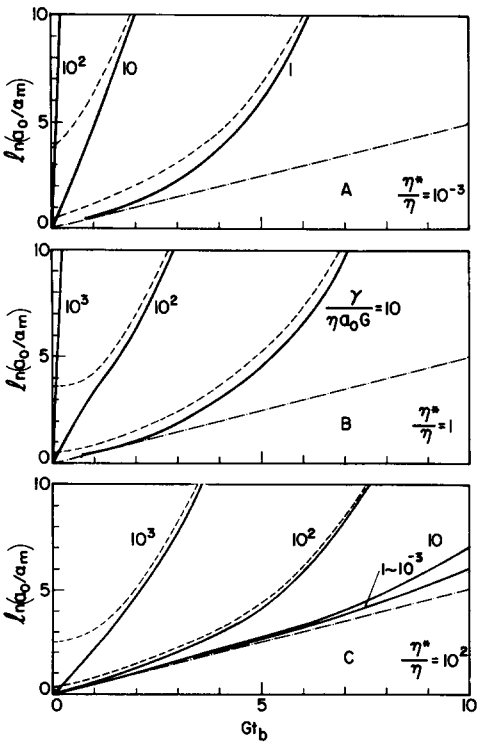

Figure 8. $\ln(a_0/\alpha_m)$ against Gt_b for (A) $\eta^*/\eta = 10^{-3}$, (B) $\eta^*/\eta = 1$, and (C) $\eta^*/\eta = 10^2$, for various $\gamma/\eta a_0 G$. The numbers designate $\gamma/\eta a_0 G$, the lines ----- the asymptotic values for large Gt_b given by [96] and the lines $-\cdot-\cdot-$ the upper bound for Gt_b given by [94].

The first term dominates as $Gt_b \to \infty$. Hence

$$\ln(\epsilon^{-1}) \sim \frac{\gamma}{\eta a_0 G} e^{Gt_b/2} K\left(\frac{\eta^*}{\eta}\right) + \frac{1}{2} Gt_b + 0(1) \qquad [96]$$

as $Gt_b \to \infty$, where

$$K\left(\frac{\eta^*}{\eta}\right) = \frac{1}{3}(y_*)^{1/3} \int_{y_*}^{1} x^{-4/3}(1-x^2)\Phi(x)\,dx$$
$$= (1-y_*^2)\Phi(y_*), \qquad [97]$$

[85] having been used.

From figure 9 it is seen that $K(\eta^*/\eta)$ is a decreasing function of η^*/η, showing that t_b increases with increasing η^*/η as already noted.

Using [96], the asymptotic values of $\ln(a_0/\alpha_m)$ were plotted as ---- lines in figure 8. The calculated relation between R/a_0 and $\ln(\epsilon^{-1})$ for various $\gamma/\eta a_0 G$ obtained from the relations between R/a_0 and Gt_b ([86]) and between $\ln(\epsilon^{-1})$ and Gt_b ([93]) are shown in figure 10 for

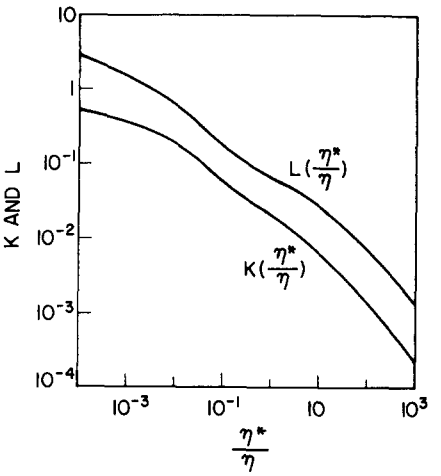

Figure 9. Functions $K(\eta^*/\eta)$ and $L(\eta^*/\eta)$ defined by [97] and [102] respectively.

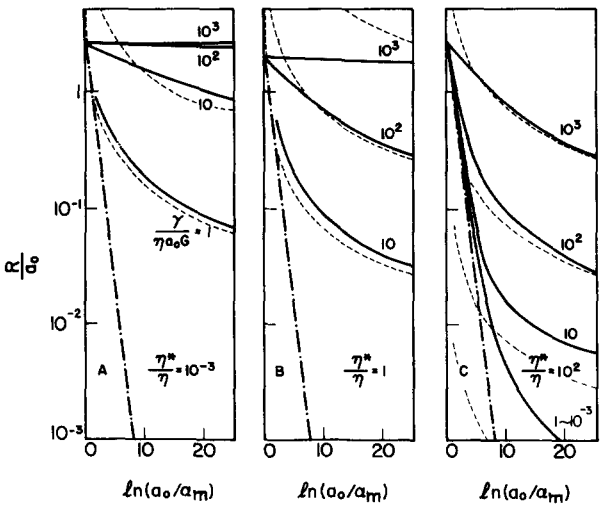

Figure 10. Relation between R/a_0 and $\ln a_0/\alpha_m$ for (A) $\eta^*/\eta = 10^{-3}$, (B) $\eta^*/\eta = 1$, and (C) $\eta^*/\eta = 10^2$, for various $\gamma/\eta a_0 G$. The numbers designate $\gamma/\eta a_0 G$, the lines ----- the asymptotic values for large Gt_b given by [101] and the lines -·-·-·-·- the lower bound for $\ln R/a_0$ given by [100].

$\eta^*/\eta = 10^{-3}$, 1.0 and 10^2. It is clear from these results, that except for very large disturbances for which ϵ is not too small, the larger η^*/η is, the smaller R/a_0 will be for a given $\eta a_0 G$ and ϵ. This means that if the liquid thread is very viscous, it will elongate to a thread of very small radius and remain stable for a long time before finally breaking up into drops of very small size. Also, smaller drops are produced by decreasing the value of $\gamma/\eta a_0 G$. A lower bound for R/a_0 may be obtained by considering the inequality $a_b > \alpha_m$ discussed previously. Using [86], we obtain

$$\frac{R}{a_0} = \left(\frac{3\pi}{2x_{opt}}\right)^{1/3} \frac{a_b}{a_0} > \left(\frac{3\pi}{2x_{opt}}\right)^{1/3} \frac{\alpha_m}{a_0}. \qquad [98]$$

Hence

$$\ln \frac{R}{a_0} > \frac{1}{3} \ln \left(\frac{3\pi}{2x_{opt}}\right) - \ln \left(\frac{a_0}{\alpha_m}\right). \qquad [99]$$

The values of x_{opt} for all η^*/η and $\gamma/\eta a_0 G$ would, from our theoretical calculations, appear to be bounded above by the maximum value 0.589 obtained from the case of the stationary liquid cylinder by Tomotika. If this is true, then

$$\ln \frac{R}{a_0} > \frac{1}{3} \ln \left(\frac{3\pi}{1.178}\right) - \ln \left(\frac{a_0}{\alpha_m}\right). \qquad [100]$$

This lower bound is plotted in figure 10 as -·-·-·- line. For $Gt_b \to \infty$, we obtain from [87] and [96]

$$\frac{R}{a_0} \sim \frac{\gamma}{\eta a_0 G} (\ln \epsilon^{-1})^{-1} L\left(\frac{\eta^*}{\eta}\right), \qquad [101]$$

where

$$L\left(\frac{\eta^*}{\eta}\right) = \left(\frac{3\pi}{2}\right)^{1/3} (y_*)^{-1/3} (1 - y_*^2) \Phi(y_*). \qquad [102]$$

Asymptotic values calculated from [101] are plotted in figure 10 as ----- lines. The function $L(\eta^*/\eta)$, plotted in figure 9 is a decreasing function of η^*/η, showing that R/a_0 is a decreasing function of η^*/η as already noted.

EXPERIMENTAL

1. *General*

While the theory described above applies to axisymmetric extensional flow, experiments were performed using plane hyperbolic flow, conducted in a "four-roller" apparatus the same as that of Rumscheidt & Mason (1961a). This discrepancy between the flows in the theory and experiment will be discussed later. Between the four vertical rollers of the apparatus, the viscous suspending fluid was floated on a layer of an immiscible liquid of higher density and much lower viscosity to eliminate the effect of drag exerted by the bottom of the container.

Relative to X', Y', Z' axes with origin at centre of apparatus with the X'-axis chosen along the direction of maximum extension and the Y'-axis along the maximum contraction, the flow field produced by the rotating rollers may in the central region, be described as

$$U_x' = GX', \quad U_y' = -GY', \quad U_z' = 0, \qquad [103]$$

where U_x', U_y' and U_z' are respectively the X'-, Y'- and Z'-components of velocity, G being the extension rate.†

Following the method used by Taylor (1934), the hyperbolic flow was calibrated by measuring

†The quantity G defined here is 1/2 that used by Rumscheidt & Mason (1962).

the time needed for a tracer particle to move some given projected distance on the X'-axis and also the rotation speed N of the rollers by means of a self-timing tachometer. It was found that the value of the extension rate G so obtained was linearly proportional to N with

$$G = 9.71 \times 10^{-3} N \quad \text{For 4.0 cm dia rollers,}$$
$$G = 2.52 \times 10^{-2} N \quad \text{For 6.0 cm dia rollers,}$$

N being measured in rev/min with G in $\sec^{-1}$.

A single drop of the fluid to be pulled out into a thread was put in the suspending fluid close to the central position by direct injection from a syringe through a hypodermic needle, the diameter of drop ranging from 4 mm to 8 mm. After the apparatus was started and a good symmetrical drop elongation obtained, the subsequent decrease in thread radius and final breakup were observed by means of a microscope and a Bolex 16 mm cine-camera at a film speed of 32 frames per sec, the viewing direction being parallel to the axes of the rollers. Accurate film speeds were obtained by measuring the time of film run and comparing it with the number of frames which were indicated on the camera.

A frame-by-frame analysis of the film gave the liquid thread radius and the wave length of the surface wave just before breakup. Overall magnification upon projection of the film was about 89×.

The apparatus was operated at a room temperature of 23 ± 0.5°C.

2. *Materials*

Castor oil (Fischer Scientific Co.) was used as the suspending phase which was floated on water with sugar added to increase density.

Silicone oils of 100cs and 1000cs (Dow Corning fluid 200) were used as drop phase, the properties of these materials being shown in table 1.

Table 1. Properties of materials (temperature at 23°C)

System No.	Drop phase	Continuous phase	η^* (poise)	η (poise)	η^*/η	ρ^* (g/cm^3)	ρ (g/cm^3)	γ (dyne/cm)
1.	Silicone oil 1000 cs	Castor oil	10.7	7.28	1.46	0.973	0.959	5.2
2.	Silicone oil 100 cs	Castor oil	1.08	7.28	0.148	0.968	0.959	4.6

Note: ρ^* and ρ are densities of drop and continuous phase.

RESULTS AND DISCUSSION

It was observed that breakup under extension of the liquid thread is characterized by the formation of large drops connected by thin liquid filaments, which on further extension develop a secondary varicosity and break up, leaving a myriad of satellite droplets between the larger principal drops. Furthermore, in contrast to the breakup of a stationary liquid thread (Rumscheidt & Mason 1962), breakup under extension does not occur simultaneously over the entire length of the thread, the spacing between principal drops is not constant and the filaments do not give rise to the same number of droplets. Thus the breakup products in this case lack uniformity in size.

The decrease in the thread radius with time of extension is illustrated in figure 11, a linear variation of log a with time, as predicted by [40], being obtained. Liquid threads could usually be stretched until the thread radii were below 0.01 cm, after which breakup occurred.

The values of G calculated from the slopes of the lines in figure 11 using [40] were compared with those which were obtained by the tracer method explained previously. Results are shown by closed circles in figure 12. There is some difference between these values of G, especially for larger values of the extension rate. One possible explanation for this is that because plane

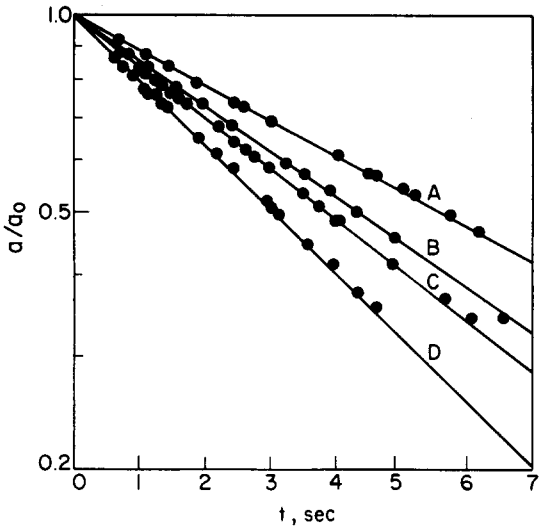

Figure 11. Linear variation of $\ln a/a_0$ with time for four values of N; (A) 25 rev/min, (B) 30 rev/min, (C) 34 rev/min, (D) 40 rev/min. Suspending phase is castor oil and extending thread phase is silicone oil of 100 cs.

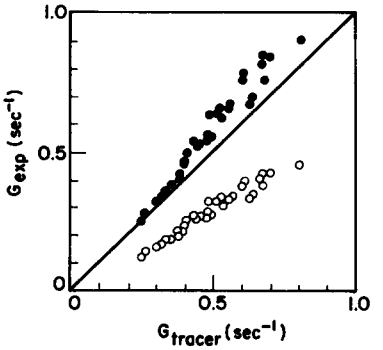

Figure 12. Comparison of G_{tracer} obtained by tracer particle method with G_{exp} obtained from experimental measurements of thread radius (i) by the use $a/a_0 = e^{-Gt/2}$ [40] indicated by closed circles, and (ii) by the use of $a/a_0 = e^{-Gt}$ indicated by open circles.

hyperbolic flow is being used the liquid thread undergoing extension might be slightly more compressed in the direction of the Y'-axis than in the direction of the Z'-axis, the liquid thread no longer being of circular cross-section. However, due to interfacial tension trying to make the thread cross-section circular, considerable reduction of thread dimension in the Z'-direction from the initial value a_0 is to be expected. In fact, if the experimental results in figure 11 are used to compute G by using the result $a/a_0 = e^{-Gt}$ for no compression in the Z'-direction (rather than the result of $a/a_0 = e^{-Gt/2}$), the values obtained (shown by open circles in figure 12) show a very large error when compared with values of G obtained by tracer particles. This suggests that the flow close to the extending thread is approximately an axisymmetric extensional flow rather than a plane hyperbolic flow, and that the theory described in the previous sections may be expected to apply. A detailed discussion of the flow around a thread in a plane hyperbolic flow is given in appendix III, where it is shown theoretically that for the present experiments the thread has an approximately circular cross-section, its stability being essentially the same as that of a thread in axisymmetric extensional flow.

We next measured the wavelength of the principal wave, λ_b just before breakup of liquid thread. The thread radius at breakup a_b was calculated from [40] using the value of G calibrated by the tracer particle method and measured values of a_0 and t_b. This time to breakup, t_b, was measured from an initial time (at which $a = a_0$) chosen not too long after application of extensional flow, so that waves would not already have been amplified, and also not too soon

after application of flow, so that one would have a uniform liquid thread. The experimentally obtained breakup time, t_b and breakup radius a_b were plotted against G in figure 13A and B respectively for System 1 ($\eta^*/\eta = 1.46$, $\gamma = 4.6$) and System 2 ($\eta^*/\eta = 0.148$, $\gamma = 4.6$). Both t_b and a_b decrease with increase of G, a_b for System 2 being larger than that for System 1. Thus as indicated by the theory (see figure 10) the larger the viscosity ratio η^*/η, the more stable the liquid cylinder and the smaller the value of a_b.

Both measured values and calculated theoretical values of $2\pi a_b/\lambda_b$ vs Gt_b are shown in figure 14 for Systems 1 and 2. Although the experimental values were scattered around the theoretical values, the agreement is considered to be good. The reason for the scatter of the data might be due to the fact that the wavelength at the breakup point was not so regular and reproducible as for the case where there was no extensional flow.

The theory can predict the wave number $2\pi a_b/\lambda_b$ at breakup and hence the resulting drop diameter if the values of η^*/η, $\gamma/\eta a_0 G$ and $\ln a_0/\alpha_m$ are known. As shown in figure 10, large η^*/η and small $\gamma/\eta a_0 G$ are better for getting smaller R/a_0 at fixed $\ln a_0/\alpha_m$. For given fluid properties and extension rate, one requires the value of α_m, the disturbance amplitude to evaluate R/a_0. For the breakup of a stationary liquid thread (Rumscheidt & Mason 1962) the value of α_m is of the order of $10^{-5} \sim 10^{-6}$ cm. On the other hand, Kuhn (1953) considered the case where these initial disturbances come from thermal fluctuations only and found that, for a jet of Newtonian fluid, α_m is

$$\alpha_m = \sqrt{\left(\frac{21kT}{8\pi^{3/2}\gamma}\right)}, \qquad [104]$$

where k is Boltzmann's constant, T the absolute temperature, and γ the surface tension. This gives values of α_m in the range 10^{-7}–10^{-8} cm. The calculated values of $\ln a_0/\alpha_m$ from the present experimental results (i.e. from the values of Gt_b shown in figure 13) were in the range 8.8–12.0. Since a_0 was of the order of 0.1 cm, this yielded α_m in the range 6.6×10^{-7}–1.5×10^{-5} cm.

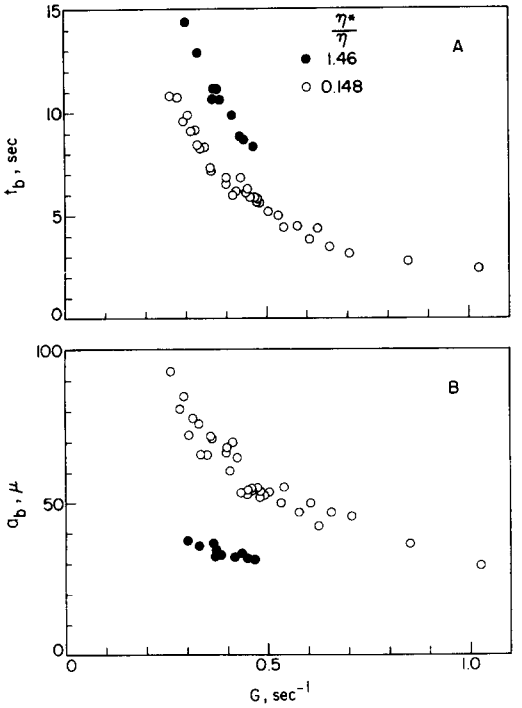

Figure 13. (A) Experimentally obtained breakup time t_b vs extension rate G for System 1 (solid circles, $\eta^*/\eta = 1.46$, $\gamma = 5.2$) and System 2 (open circles, $\eta^*/\eta = 0.148$, $\gamma = 4.6$). (B) Experimentally obtained breakup radius a_b of liquid thread vs extension rate G. All points correspond to those in (A).

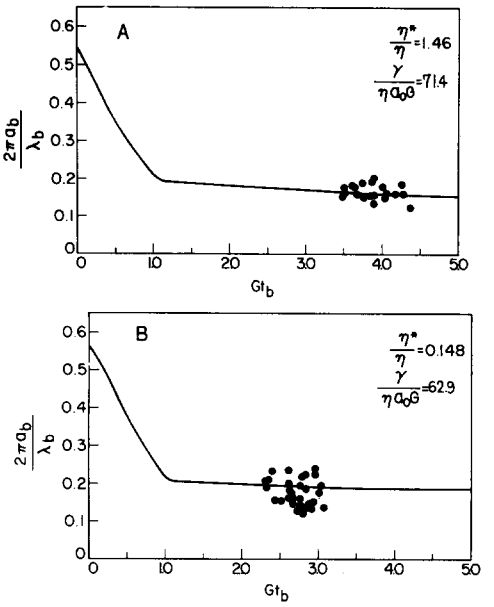

Figure 14. Theoretical (line) and experimental (point) wave numbers at breakup as functions of Gt_b for (A) Systems 1 and (B) System 2.

For all experiments performed, the Reynolds number, $a_0^2 G/\nu$ was very small (of order 10^{-3}), this being a necessary condition for the theory to apply.

As mentioned before, it was observed that during the breakup of the extending liquid thread, drops connected by thin liquid filaments are formed, these filaments themselves then breaking up to a myriad of satellite droplets between the larger principal drops. Thus the actual average particle radius will be smaller than that predicted by this theory. For this reason we did not measure drop size in experiments to confirm the theory. However, it is seen from figure 10 that the requirements for producing drops of small size by applying extensional flow to a liquid thread are that (i) the viscosity ratio η^*/η is large and (ii) the parameter, $\gamma/\eta a_0 G$ is small. For example, if we chose $\eta^*/\eta = 10^2$, $\gamma/\eta a_0 G = 1$, and $a_0 = 10^{-2}$ cm, and assume $\alpha_m = 10^{-6}$ cm, we get $R/a_0 = 5 \times 10^{-3}$, the values of $R = 0.5\mu$ being obtained. This gives $G(\sec^{-1}) = (\gamma/\eta) \times 10^2$ and $t_b(\sec) = 13.3 \times 10^{-2}\ \eta/\gamma$ where the units of η and γ are poise and dyne/cm respectively. It should be noted that for the theory to apply the value of $\gamma/\eta a_0 G$ should not be too large, otherwise the drop would never be pulled into a liquid thread.

In the axisymmetric extensional flow the line of fluid particles through the drop centre which is extending at the greatest rate, namely that parallel to the z-axis, remains in that direction as long as the flow continues. Thus the stress due to the viscous drag of the suspending medium is therefore always tending to further extend the liquid thread in the same direction. However, in a shear flow, the line of particles which lie in the direction of maximum rate of extension, namely at 45° to the direction of flow is continually being rotated away from that position.

In fact, when the viscosity ratio η^*/η is very large, a drop in a shear flow will rotate almost like a solid body, lines of particles in it extending slowly while they are within 45° of the direction of maximum rate of extension and contracting slowly while they are within 45° of the direction of maximum rate of contraction. Hence the drop experiences very little deformation and will not break up at all if η^*/η is greater than approximately 3.6, however large the shear rate may be (Rumscheidt & Mason 1961b; Torza *et al.* 1972). Thus for large η^*/η, an extensional flow is very much more effective in producing very small drops than a shear flow.

REFERENCES

GOLDSMITH, H. L. & MASON, S. G. 1963 The flow of suspensions through tubes II. Single large bubbles. *J. Colloid Sci.* **18**, 237–261.

GOREN, S. L. 1962 The instability of an annular thread of fluid. *J. Fluid Mech.* **12**, 309–319.

GOREN, S. L. 1964 The shape of a thread of liquid undergoing break-up. *J. Colloid Sci.* **19**, 81–86.

KUHN, W. 1953 Spontane Aufteilung von Flüssigkeitszylindern in kleine Kugeln. *Kolloid Z.* **132**, 84–99.

RUMSCHEIDT, F. D. & MASON, S. G. 1961a Particle motions in sheared suspensions. XI. Internal circulation in fluid drops (experimental). *J. Colloid Sci.* **16**, 210–237.

RUMSCHEIDT, F. D. & MASON, S. G. 1961b Particle motions in sheared suspensions. XII. Deformation and burst of fluid drops in shear and hyperbolic flow. *J. Colloid Sci.* **16**, 238–261.

RUMSCHEIDT, F. D. & MASON, S. G. 1962 Break-up of stationary liquid threads. *J. Colloid Sci.* **17**, 260–269.

TAYLOR, G. I. 1934 The formation of emulsions in definable fields of flow. *Proc. R. Soc.* **A146**, 501–523.

TOMOTIKA, S. 1935 On the instability of a cylindrical thread of a viscous liquid surrounded by another viscous fluid. *Proc. R. Soc.* **A150**, 322–337.

TOMOTIKA, S. 1936 Breaking up of a drop of viscous liquid immersed in another viscous fluid which is extending at a uniform rate. *Proc. R. Soc.* **A153**, 302–318.

TORZA, S., COX, R. G. & MASON, S. G. 1972 Particle motions in sheared suspensions. XXVII. Transient and steady deformation and burst of liquid drops. *J. Colloid Sci.* **38**, 395–411.

APPENDIX I: ASYMPTOTIC FORMS OF $\Phi(x)$ AND $\bar{\Phi}(x)$

[I-A] The series expansions of the modified Bessel functions correct to $0(x^5)$ about $x = 0$,

$$I_0(x) \sim 1 + \frac{1}{4}x^2 + \frac{1}{64}x^4$$

$$I_1(z) \sim \frac{1}{2}x + \frac{1}{16}x^3 + \frac{1}{384}x^5,$$

$$K_0(x) \sim -\left(\gamma + \ln\frac{1}{2}x\right)\left(1 + \frac{1}{4}x^2 + \frac{1}{64}x^4\right) + \left(\frac{1}{4}x^2 + \frac{3}{128}x^4\right),$$

$$K_1(x) \sim x^{-1} + \left(\gamma + \ln\frac{1}{2}x\right)\left(\frac{1}{2}x + \frac{1}{16}x^3 + \frac{1}{384}x^5\right) - \left(\frac{1}{4}x + \frac{5}{64}x^3 + \frac{5}{1152}x^5\right),$$

when substituted into [57] and [58], yield

$$\Phi(x) \sim -x\left(\frac{\eta}{\eta^*}\right)\left\{\left(\frac{1}{2}x + 0(x^3)\right)(-x^{-2} + 0(\ln x)) - \left(\frac{1}{2}x + 0(x^3)\right)(-x^{-2} + 0(\ln x))\right\},$$
$$\sim 0(x^2 \ln x), \qquad \text{[I-1]}$$

$$\bar{\Phi}(x) \sim x^2 \ln\frac{1}{2}x \quad \text{as } x \to 0. \qquad \text{[I-2]}$$

[I-B] The asymptotic expansions of the modified Bessel functions for large x are

$$I_0(x) \sim \frac{e^x}{\sqrt{(2\pi x)}}\left(1 + \frac{1}{8x} + \frac{9}{128x^2} + \frac{75}{1024x^3} + \cdots\right),$$

$$I_1(x) \sim \frac{e^x}{\sqrt{(2\pi x)}}\left(1 - \frac{3}{8x} - \frac{15}{128x^2} - \frac{105}{1024x^3} + \cdots\right),$$

$$K_0(x) \sim \sqrt{\left(\frac{\pi}{2x}\right)}e^{-x}\left(1 - \frac{1}{8x} + \frac{9}{128x^2} - \frac{75}{1024x^3} + \cdots\right),$$

$$K_1(x) \sim \sqrt{\left(\frac{\pi}{2x}\right)}e^{-x}\left(1 + \frac{3}{8x} - \frac{15}{128x^2} + \frac{105}{1024x^3} + \cdots\right),$$

which when substituted into [57] and [58] yield

$$\Phi(x) \sim \left(1+\frac{\eta^*}{\eta}\right)^{-1} x^{-1}, \qquad \text{[I-3]}$$

$$\bar{\Phi}(x) \sim -\frac{1}{2}\left(1+\frac{\eta^*}{\eta}\right)^{-1} x^{-1} \quad \text{as } x \to \infty. \qquad \text{[I-4]}$$

APPENDIX II: NUMERICAL CALCULATION OF THE RELATIVE AMPLITUDE EQUATION

For convenience of numerical integration, the integrands in [65] were divided into the two terms

$$\int_x^{x_0} F(x)\,dx = \int_x^1 F(x)\,dx - \int_{x_0}^1 F(x)\,dx, \qquad \text{[II-1]}$$

the integrals being evaluated by the Runge–Kutta method. Due to the necessity of evaluation for large x_0, the second integral was evaluated numerically up to $x = 40$, the remaining part $(40 < x < x_0)$ being obtained analytically from the asymptotic form of the integrand (derived from the asymptotic forms of $\Phi(x)$ and $\bar{\Phi}(x)$ given in [66] and [67]. That the exact and asymptotic forms of Φ and $\bar{\Phi}$ are almost identical for $x > 40$ is shown in figure 15.

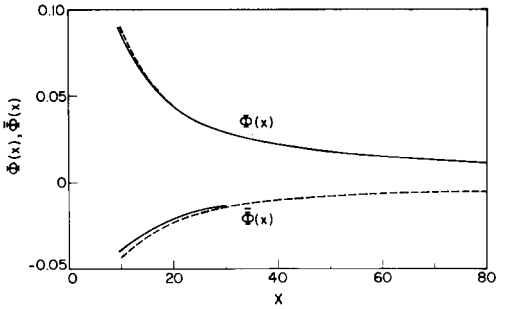

Figure 15. Comparison of exact (solid line) and asymptotic (broken line) values for $\Phi(x)$ and $\bar{\Phi}(x)$.

Thus for $x_0 > 40$ and $x < 40$, [65] is approximated by

$$\ln(\alpha/\alpha_0) = \frac{\gamma x_0^{1/3}}{3\eta a_0 G}\left[\int_x^{40} x^{-4/3}(1-x^2)\Phi(x)\,dx - \frac{3}{2}\left(1+\frac{\eta^*}{\eta}\right)^{-1}(x_0^{2/3} - 40^{2/3})\right]$$

$$-\left(\frac{\eta^*}{\eta}-1\right)\left[\int_x^{40} x^{-1}\bar{\Phi}(x)\,dx + \frac{1}{2}\left(1+\frac{\eta^*}{\eta}\right)^{-1}(x_0^{-1} - 40^{-1})\right] + \frac{1}{3}\ln\frac{x}{x_0}. \qquad \text{[II-2]}$$

APPENDIX III: LIQUID THREAD IN PLANE HYPERBOLIC FLOW

Relative to the cylindrical polar coordinates shown in figure 1, a plane hyperbolic flow in the $\phi = 0$ plane with maximum extension rate G in the z-direction may be represented as

$$\begin{aligned} u_r &= -Gr\cos^2\phi, \\ u_\phi &= +Gr\sin\phi\cos\phi, \\ u_z &= +Gz. \end{aligned} \qquad \text{[III-1]}$$

This may be expressed as the sum of two flows,

$$\mathbf{u} = \mathbf{u}' + \mathbf{u}'', \qquad \text{[III-2]}$$

where $\mathbf{u}'$ is the axisymmetric extensional flow

$$u'_r = -\frac{1}{2}Gr, \quad u'_\phi = 0, \quad u'_z = +Gz, \tag{III-3}$$

and $\mathbf{u}''$ is a flow in planes perpendicular to the z-axis,

$$u''_r = -\frac{1}{2}Gr\cos 2\phi, \quad u''_\phi = +\frac{1}{2}Gr\sin 2\phi, \quad u''_z = 0. \tag{III-4}$$

A thread of fluid suspended in the flow $\mathbf{u}'$ has already been examined. We will therefore examine the effect of the flow $\mathbf{u}''$ on the thread which is assumed to have an approximately circular cross-section given by

$$r = a + f(\phi), \tag{III-5}$$

where $f(\ll a)$ is a function of ϕ only. The flow $\mathbf{u}^*$ inside and $\mathbf{u}$ outside the thread due to $\mathbf{u}''$ satisfies the creeping motion equations with

$$\mathbf{u} \sim \mathbf{u}'', \quad \text{as } \mathbf{r} \to \infty, \tag{III-6}$$

with the boundary conditions on the surface being:

(i) Zero normal velocity

$$u_r = u^*_r = 0 \quad \text{on } r = a, \tag{III-7}$$

(ii) Continuity of tangential velocity

$$u_\phi = u^*_\phi \quad \text{on } r = a, \tag{III-8}$$

(iii) Continuity of tangential stress

$$\eta\left(\frac{\partial u_\phi}{\partial r} + \frac{1}{r}\frac{\partial u_r}{\partial \phi} - \frac{u_\phi}{r}\right) = \eta^*\left(\frac{\partial u^*_\phi}{\partial r} + \frac{1}{r}\frac{\partial u^*_r}{\partial \phi} - \frac{u^*_\phi}{r}\right) \quad \text{on } r = a, \tag{III-9}$$

(iv) Balance of normal hydrodynamic stress by interfacial tension

$$-\left(-p^* + 2\eta^*\frac{\partial u^*_r}{\partial r}\right) + \left(-p + 2\eta\frac{\partial u_r}{\partial r}\right) = \frac{\gamma}{a + f + \dfrac{\mathrm{d}^2 f}{\mathrm{d}\phi^2}} \quad \text{on } r = a, \tag{III-10}$$

where p^* and p are the pressures fields corresponding to $\mathbf{u}^*$ and $\mathbf{u}$ respectively. Defining a stream function ψ^* inside the thread by the relations

$$u^*_r = \frac{1}{r}\frac{\partial \psi^*}{\partial \phi}, \quad u^*_\phi = -\frac{\partial \psi^*}{\partial r}, \tag{III-11}$$

and the stream function ψ outside the thread similarly, it is seen that ψ^* and ψ satisfy equations of the form

$$\left[\frac{1}{r}\frac{\partial}{\partial r}\left(r\frac{\partial}{\partial r}\right) + \frac{1}{r^2}\frac{\partial^2}{\partial \phi^2}\right]^2 \psi^* = 0. \tag{III-12}$$

From the value of $\mathbf{u}''$ given in [III-4], the boundary condition [III-6] may be written as

$$\psi \sim -\frac{1}{4}Gr^2 \sin 2\phi \quad \text{as } r \to \infty. \tag{III-13}$$

Thus assuming ψ and ψ^* to be proportional to $\sin 2\phi$ the solution of [III-12] gives

$$\psi^* = (Cr^2 + Dr^4)\sin 2\phi,$$

$$\psi = \left(-\frac{1}{4}Gr^2 + A + Br^{-2}\right)\sin 2\phi, \tag{III-14}$$

where A, B, C, D are constants and where boundary condition [III-13] and the requirement that $\mathbf{u}^*$ be bounded at $r = 0$ have been used. Substituting these values of ψ^* and ψ into the boundary conditions [III-7,8,9], the values of A, B, C and D may be obtained to give

$$\psi^* = G \sin 2\phi\left(\frac{\eta}{4(\eta + \eta^*)}r^2 - \frac{\eta}{4(\eta + \eta^*)}a^{-2}r^4\right),$$

$$\psi = G \sin 2\phi\left(-\frac{1}{4}r^2 + \frac{(\eta + 2\eta^*)}{4(\eta + \eta^*)}a^2 - \frac{\eta^*}{4(\eta + \eta^*)}a^4 r^{-2}\right). \tag{III-15}$$

Obtaining the values of $\mathbf{u}^*$ and $\mathbf{u}$ from [III-11] and substituting into the creeping motion equations gives the corresponding pressure fields p^* and p as

$$p^* = -\frac{3\eta^*}{\eta + \eta^*}a^{-2}r^2 G\eta \cos 2\phi + \text{constant},$$

$$p = \frac{\eta + 2\eta^*}{\eta + \eta^*}a^2 r^{-2} G\eta \cos 2\phi + \text{constant}. \tag{III-16}$$

The normal stress boundary condition [III-10] upon substitution of the values of p, p^*, $\mathbf{u}$ and $\mathbf{u}^*$, gives

$$-3G\eta \cos 2\phi + \text{constant} = \frac{\gamma}{a + f + \dfrac{d^2 f}{d\phi^2}}. \tag{III-17}$$

Since $f \ll a$

$$-3G\eta \cos 2\phi + \text{constant} = \frac{\gamma}{a} - \frac{\gamma}{a^2}\left(f + \frac{d^2 f}{d\phi^2}\right). \tag{III-18}$$

Hence

$$\frac{d^2 f}{d\phi^2} + f = \frac{3G\eta a^2}{\gamma}\cos 2\phi, \tag{III-19}$$

giving

$$f = -\frac{G\eta a^2}{\gamma}\cos 2\phi. \tag{III-20}$$

Thus the cross-sectional shape of the thread is

$$r = a\left(1 - \frac{G\eta a}{\gamma}\cos 2\phi\right). \tag{III-21}$$

As a measure of the deformation of the cross-sectional shape from circular we define a quantity

$$D = \frac{L - B}{L + B}, \qquad \text{[III-22]}$$

where $L = 2a[1 + (G\eta a)]$ is the maximum and $B = 2a[1 - (G\eta a/\gamma)]$ is the minimum distance across the thread cross-section. Thus

$$D = \frac{G\eta a}{\gamma} = \frac{G\eta a_0}{\gamma} e^{-Gt/2}, \qquad \text{[III-23]}$$

so that at large times, the cross-section becomes circular. In the experiments performed here, the value of D calculated from [III-23] decreased from 1.4×10^{-2} to 1.9×10^{-3} for System 1 and from 1.6×10^{-2} to 3.9×10^{-3} for System 2 as t increased from 0 to t_b. Hence the effect of the deformation from circular of the cross-section should be negligible.

Furthermore, if one includes the flow fleld $\mathbf{u}''$ in the stability analysis, the boundary conditions [18], [30] and [35] are unaltered if one again considers disturbances of the form given by [12]. This means that the stability of a thread in plane hyperbolic flow given by [III-1] is identical to that of a thread in the axisymmetric extensional flow [III-3] provided of course that D given by [III-23] remains small (at least over a major fraction of time from $t = 0$ to $t = t_b$) as in the present experiments.

Résumé—On étudie théoriquement et expérimentalement la stabilité et la rupture d'un filet cylindrique de liquide visqueux en extension, suspendu dans un liquide visqueux non miscible soumis à un écoulement avec extension.

On montre que les perturbations créées à la formation du filet sont en général, lorsque le temps s'écoule, amorties, puis amplifiées et finalement amorties à nouveau. En considérant que des perturbations sont constamment apportées au système, on trouve ainsi que la perturbation qui domine à un instant donné est complètement différente de celle qui domine à tout autre instant. En admettant que la rupture advient quand l'amplitude de la perturbation atteint le rayon du cylindre, on obtient le temps de rupture et la taille finale des gouttes résultant de la rupture en fonction des propriétés des fluides, du taux d'extension et de l'amplitude des perturbations apportées au système.

Ces résultats ont été confirmés par l'examen, au moyen de la cinématographie, de la rupture d'un filet liquide dans un écoulement hyperbolique.

Auszug—Die Stabilitaet und der Zerfall eines sich ausdehnenden zylindrischen Fadens zaeher Fluessigkeit, der in einer nicht mischbaren zaehen Fluessigkeit mit Dehnungsstroemung schwebt, wird theoretisch und experimentell untersucht.

Es zeigt sich, dass die bei Bildung des Fadens ausgeloesten Stoerungen im allgemeinen im Laufe der Zeit zuerst gedaempft, spaeter verstaerkt, und schliesslich wieder gedaempft werden. Eine Betrachtung von dem System kontinuierlich zugefuehrten Stoerungen zeigt, dass eine momentan vorherrschende Stoerung von den zu anderen Zeiten auftretenden voellig verschieden ist. Unter der Annahme, dass der Zerfall geschieht, wenn die Stoerungsamplitude dem Zylinderradius gleich wird, werden Ergebnisse fuer die Zeit bis zum Zerfall und die resultierende Tropfenendgroesse erhalten, in Abhaengigkeit von den Fluessigkeitseigenschaften, der Ausdehnungsgeschwindigkeit und der dem System aufgepraegten Stoerungsamplitude.

Zur Bestaetigung der Ergebnisse wurde mit Hilfe von Kinematographie der Zerfall eines Fluessigkeitsfadens hyperbolischer Form beobachtet.

Резюме—Выполнены теоретические и экспериментальные исследования устойчивости и распада вытягивания вязкой жидкой цилиндрической нити, взвешенной во невзаимодействующем вязком жидком потоке, производящем вытяжку.

Показано, что возмущения, вызванные формированием нити, будут по мере времени тормозиться, затем усиляться, а в конце вновь затухать. При рассмотрении помех, постоянно приложенных к системе, найдено, что преобладающая в данный момент помеха совершенно отличается от той, которая преобладает в какой-либо другой момент. Предполагая, что распад происходит при достижении амплитудой помехи значения радиуса цилиндра, получены выражения для времени распада и для конечного размера капли, вытекающие из условий распада, зависящих от свойств жидкости, скорости вытягивания и амплитуды помехи, приложенной к системе.

Эти разультаты были подтверждены исследованием распада жидкой нити в гиперболизированном потоке посредством киносъемки.